PHYSICAL REVIEW D **90,** 022003 (2014)

Synthetic streams in a gravitational wave inspiral search with a multidetector network

K. Haris[*] and Archana Pai[†]

Indian Institute of Science Education and Research Thiruvananthapuram, CET Campus, Trivandrum 695016, India

(Received 2 February 2014; published 17 July 2014)

A gravitational wave inspiral search with a global network of interferometers when carried in a phase coherent fashion mimics a search with two *effective* synthetic data streams. The streams are constructed by the linear combination of the overwhitened data from individual detectors. We demonstrate here that the two synthetic data streams pertaining to the two polarizations of the gravitational wave can be derived prior to the maximum-likelihood analysis in a most natural way using the technique of singular-value decomposition applied to the *network signal-to-noise ratio vector*. The singular-value technique combined with the matched filtering in network plus spectral space enables the construction of the synthetic streams. We further show that the network log likelihood ratio is then the sum of the log-likelihood ratios of these synthetic streams. In this formalism, the four extrinsic parameters of the nonspinning inspiral signal, namely, amplitude, initial phase, binary inclination, and the polarization $\{A_0, \phi_a, \epsilon, \Psi\}$, are mapped to the two amplitudes and two phases, namely, $\{\boldsymbol{\rho}_L, \boldsymbol{\rho}_R, \Phi_L, \Phi_R\}$. We show that the maximization over the new extrinsic parameters is a straightforward exercise closely linked to the single detector approach in the literature. Toward the end, we connect all the previous works related to the multidetector gravitational wave inspiral search and present in the same notation.

DOI: 10.1103/PhysRevD.90.022003 PACS numbers: 04.80.Nn, 07.05.Kf, 95.55.Ym

I. INTRODUCTION

A global network of broadband advanced gravitational wave (GW) detectors such as Advanced LIGO and Advanced Virgo [1,2] will be ready in next few years. Japanese detector KAGRA is under construction and will be functioning in the next decade [3]. In addition, there is a proposal for a detector in India, namely, LIGO-India. Coalescing compact binaries are promising sources for these advanced detectors. These detectors with an individual average distance reach of 200 Mpc for neutron star binaries would detect few GW inspiral events per month [1,4].

The inspiral search for the compact binary (with component masses m_1 and m_2) is carried out by a phase matching technique well known as the matched filtering applied to the output data from a single detector. The inspiral signal is characterized by many physical parameters; for example, in case of nonspinning inspiraling binaries, the parameter space is $(\mathcal{M}, \eta, \mathrm{A}_0, t_a, \phi_a)$. Here, ϕ_a is the phase of the signal at the time of arrival t_a. The mass $\mathcal{M} = (m_1 m_2)^{3/5}/(m_1 + m_2)^{1/5}$ is the chirp mass, and $\eta = m_1 m_2/(m_1 + m_2)$ is the symmetric mass ratio. A_0 is the constant overall amplitude. The detection is carried out by laying the templates in the multidimensional parameter space and then maximizing the filtered output. This is technically known as maximum likelihood ratio (MLR) analysis, which is close to optimal when signal-to-ratio is large and signal is buried in Gaussian noise [5–7].

In the global multidetector network mentioned above, each interferometer is differently oriented due to its location on the Earth's globe. Thus, they have different responses to the incoming GW from a given direction. There are two distinct ways to carry out a GW search with a network of detectors. The first one is *the coincidence approach*. In this approach, data from each interferometer is processed individually followed by a list of coincident event triggers based on the coincidence windows in the mass and time of arrival parameters [8].[1] On the contrary, the second approach, the *phase coherent search*, involves combining the inspiral signal from different detectors in a phase coherent fashion into a single effective network statistic, and a detection would be carried out by applying a threshold on it. In the literature, it has been demonstrated that the coherent search performs better than the coincidence search for coalescing binaries [9]. This is understood since the phase information is retained in the coherent approach. In this work, our main focus is the multidetector phase coherent approach.

From the coherent approach perspective, different detectors in the network respond differently, which removes the parameter degeneracy present in the single detector signal. As a result, for nonspinning binaries, the search parameter

[*]haris@iisertvm.ac.in
[†]archana@iisertvm.ac.in

[1]This was the basic nature of the coincidence search in the science run data.

space expands to $(\mathcal{M}, \eta, \mathrm{A}_0, t_a, \phi_a, \theta, \phi, \epsilon, \Psi)$, where (θ, ϕ)[2] represents the source location, ϵ is the binary inclination angle, and Ψ is the polarization angle of the binary system. To give an example, two independent detectors can measure GW polarization predicted by Einstein's general relativity, and hence the polarization becomes an explicit parameter. Similarly, at least four detectors are necessary to measure the source location by the triangulation method [10].

The multidetector coherent GW inspiral search based on the MLR analysis has been developed in the literature for more than a decade by various groups around the world [11–13]. In Ref. [11], the network log-likelihood ratio (LLR) is maximized over the four extrinsic parameters out of the above-mentioned nine total parameters; namely, $(\mathrm{A}_0, \phi_a, \epsilon, \Psi)$ were maximized using the rotation group symmetries and Gel–Fand functions. The maximized network LLR was shown to be the sum-square of the projected network correlation function vectors on the (two-dimensional) polarization plane. In Ref. [12], the coherent formalism was developed for a general case of correlated noise (to treat the noise correlation between the two LIGO-Hanford detectors). In Ref. [13], the coherent formalism was developed based on the $\mathcal{F}$ statistic [14,15], where the four physical parameters $(\mathrm{A}_0, \phi_a, \epsilon, \Psi)$ are mapped to the four amplitude parameters, namely $(\mathcal{A}_1, \mathcal{A}_2, \mathcal{A}_3, \mathcal{A}_4)$. The authors showed that the freedom of polarization angle Ψ allows one to set the dominant polarization frame in which the two GW polarizations are separable. For more reference on the dominant polarization frame, see Ref. [16]. Finally, the authors show that the MLR analysis gives two terms which can be interpreted as the matched filtering output of the two synthetic streams constructed from the output of the multiple detectors, e.g., Eq. (2.35) of Ref. [13]. For more references on the synthetic streams in the GW burst context, see Ref. [17], and for GW unmodeled chirps, see Ref. [18].

As indicated in earlier literature [11,13], the MLR analysis gives two synthetic data streams which mimic the multidetector network. The number 2 corresponds to the two polarizations in the Einstein's gravity. These synthetic streams act like the building blocks for the multi-detector coherent analysis. In electromagnetic window, techniques are developed for effectively combining data from different telescopes to improve the source localization, which is generically termed as aperture synthesis [19,20]. In particular in optical/radio windows, the signals are combined from distinct telescopes with the directional dependent coefficients or data correlated among the detector pairs to improve source localization. In the same spirit, the multidetector detector coherent analysis performed with synthesis streams can be viewed as an aperture synthesis technique in the GW window.

In this paper, we show that the synthetic streams is a natural way to combine the data streams in a phase coherent fashion and which can be constructed much before doing MLR analysis. This is obtained using the singular-value decomposition (SVD) of the multidetector *signal-to-noise ratio (SNR) vector* in a much more straightforward way. The highlights of the paper are as follows:

(1) The singular vectors of the *network SNR vector* naturally gives the *dominant polarization (DP)* frame.
(2) The new formalism imposes the simultaneous matched filtering in the spectral as well as network space and is hence termed as the *network matched filter*. This gives a pair of synthetic streams, which is similar in nature to the ones obtained in earlier literature through the MLR [13].
(3) The network LLR expressed in terms of the synthetic streams corresponding to the two singular vectors is the sum of the LLRs of the two effective synthetic data streams.
(4) In this framework, the four physical extrinsic parameters $(\mathrm{A}_0, \phi_a, \epsilon, \Psi)$ are uniquely mapped to four new parameters, namely, $(\boldsymbol{\rho}_L, \boldsymbol{\rho}_R, \Phi_L, \Phi_R)$.
(5) The network MLR amounts for maximizing the network LLR over the two effective amplitudes $(\boldsymbol{\rho}_L, \boldsymbol{\rho}_R)$ and two effective phases, (Φ_L, Φ_R). This is a clear extension of the MLR approach with single detector data stream to MLR analysis of two effective synthetic streams (corresponding to two GW polarizations). Thus, the synthetic streams effectively mimic the multidetector network search.

The approach gives an elegant way to obtain and construct the synthetic streams in multidetector analysis. Further, we connect this work to all the existing works, namely, Refs. [11,13], bringing different notations under the same umbrella.

The paper is organized as follows. Section II briefly outlines the binary signal with two polarizations in the multidetector network. In Sec. III, we define a SNR vector $\boldsymbol{\varrho}$ for which the norm is the optimal network SNR. Using the SVD technique, we show that its norm square can also be split as the sum of the two distinct quantities, $\boldsymbol{\rho}_L^2$ and $\boldsymbol{\rho}_R^2$. In Sec. IV, we obtain two synthetic streams as linear combinations of network signal such that their respective SNRs are $\boldsymbol{\rho}_L$ and $\boldsymbol{\rho}_R$. In Sec. V, we construct the network likelihood statistic, Λ in terms of synthetic streams. Further, we show that the extrinsic physical parameters are mapped into $(\boldsymbol{\rho}_L, \boldsymbol{\rho}_R, \Phi_L, \Phi_R)$. Thus, the network MLR analysis is equivalent to the MLR analysis of the two independent network synthetic streams, and the maximization is equal to maximizing the two effective amplitudes and the two effective phases. In Sec. VI, we compare our approach to the existing literature [11,13].

[2]Spherical polar coordinates (θ, ϕ) are related to the equatorial coordinates, right ascension (RA) and declination (Dec), as RA $= \phi$ and Dec $= \theta - \pi/2$.

II. INSPIRALING BINARY GW SIGNAL IN A MULTIDETECTOR NETWORK

In this section, we introduce the inspiral GW signal arriving at the network of I interferometric GW antennas.

The time series of two polarizations of GW from a nonspinning compact binary with masses m_1, m_2 and located at a distance r which enter the interferometric detector band at time t_a with the phase ϕ_a is

$$h_+(t) = \mathrm{A}(m_1, m_2, r, t)\frac{1+\cos^2\epsilon}{2}\cos\left[\Phi(t-t_a)+\phi_a\right],$$
$$h_\times(t) = \mathrm{A}(m_1, m_2, r, t)\cos\epsilon\ \sin\left[\Phi(t-t_a)+\phi_a\right], \quad (1)$$

where $\Phi(t-t_a)$ is the phase restricted to 3.5 PN order and the inclination angle ϵ is the angle between the orbital angular momentum vector and the observer's line of sight.

The corresponding strain (response) measured by any interferometric GW detector is

$$s(t) \equiv \mathrm{F}_+ h_+(t) + \mathrm{F}_\times h_\times(t), \quad (2)$$

where F_+ and $\mathrm{F}_\times$ are the antenna pattern functions which describe the angular response of an antenna to a given source location. These antenna pattern functions depend on the source location with respect to the detector's site.

In a multidetector network, we represent the antenna patterns as I-dimensional vectors, namely, $\mathbf{F}_{+,\times} = \{\mathrm{F}_{+,\times m}\}$, where the subscript m varies from 1 to I. In addition, different detectors receive the $h_{+,\times m}$ with time delays depending on the location of the detector on the Earth's globe. Thus, the signal at the mth detector site is $s_m(t) = s_{\mathrm{ref}}(t-\tau_m)$, where $s_{\mathrm{ref}}(t)$ is the GW signal in the geocentric frame, which we treat as reference here, and τ_m is the time delay between the signal in the mth detector and the geocentric frame with respect to the source location. However, for the context of this paper, henceforth we assume that we compensate for the delays and consider the delayed signal keeping the same notation to construct the network signal.[3]

The antenna pattern vectors when measured in the geocentric frame $\mathbf{F}_{+,\times}$ are the functions of the polarization angle Ψ, source location (θ, ϕ), and detector's Euler angles with respect to the geocentric frame. We use $(\alpha_m, \beta_m, \gamma_m)$ to represent the mth detector's Euler angles following the convention in the literature [11,13,18].

In the discrete domain, we express the delayed and sampled signal arrived at the mth detector with $2N$ number of time samples as a $2N$ dimensional vector,[4]

$$\mathbf{s}_m = \mathrm{F}_{+m}\mathbf{h}_+ + \mathrm{F}_{\times m}\mathbf{h}_\times \equiv \Re[\mathrm{F}^*_m\mathbf{h}], \quad (3)$$

where $\mathbf{h} = \mathbf{h}_+ + i\mathbf{h}_\times$ and $\mathrm{F}_m = \mathrm{F}_{+m} + i\mathrm{F}_{\times m}$ is the complex antenna pattern.

In the frequency domain, the signal becomes

$$\tilde{\mathbf{s}}_m = \mathrm{F}_{+m}\tilde{\mathbf{h}}_+ + \mathrm{F}_{\times m}\tilde{\mathbf{h}}_\times, \quad (4)$$

where N-dimensional vectors $\tilde{\mathbf{h}}_+$ and $\tilde{\mathbf{h}}_\times$ are the discrete versions of frequency domain GW polarizations $\tilde{h}_+(f)$ and $\tilde{h}_\times(f)$ for the positive frequencies. From Eq. (1), it can be shown[5] that

$$\tilde{h}_+(f) = \mathrm{A}_0\frac{1+\cos^2\epsilon}{2}h_0(f)e^{i\phi_a},$$
$$\tilde{h}_\times(f) = \mathrm{A}_0\cos\epsilon\ h_{\pi/2}(f)e^{i\phi_a}, \quad (5)$$

with $\tilde{h}_0(f) = i\tilde{h}_{\pi/2}(f) = f^{-7/6}e^{i\varphi(f)}$, the stationary phase approximated frequency domain waveform. Here A_0 is the constant which depends on the masses and the distance, and $\varphi(f)$ is the 3.5 PN corrected phase of the inspiral signal [22]. In the coming sections, we use $\tilde{\mathbf{h}}_0$ and $\tilde{\mathbf{h}}_{\pi/2}$ to represent discrete versions of $\tilde{h}_0(f)$ and $\tilde{h}_{\pi/2}(f)$, respectively.

Thus, the incoming signal to a multidetector network of I interferometric detectors with N number of frequency samples expressed as a $N \times I$ matrix,

$$\tilde{\boldsymbol{\mathcal{S}}}_{N\times I} \equiv [\tilde{\mathbf{s}}_1\tilde{\mathbf{s}}_2\ldots\tilde{\mathbf{s}}_I]. \quad (6)$$

III. NETWORK SNR

We assume the noises in individual detectors to be independent, additive, stationary Gaussian. Thus, the network optimal SNR square is the sum of squares of optimal SNRs of the individual detectors [11,13,18] as

$$\boldsymbol{\rho}^2 = \sum_{m=1}^{I}\rho_m^2 = 4\sum_{m=1}^{I}\left[\sum_{j=1}^{N}\frac{|\tilde{\mathcal{S}}_{jm}|^2}{\mathcal{N}_{jm}}\right],$$
$$= \mathrm{A}_0^2\left[\sum_{m=1}^{I} g_m^2\mathrm{F}_{+m}^2\left(\frac{1+\cos^2\epsilon}{2}\right)^2 + g_m^2\mathrm{F}_{\times m}^2\cos^2\epsilon\right], \quad (7)$$

where $\mathcal{N}_{jm}$ is the jth frequency component of one sided noise power spectral density (PSD) vector of mth antenna[6] [23] and $g_m^2 = \langle\mathbf{h}_0|\mathbf{h}_0\rangle_m$.[7] Here subscript m denotes the noise PSD of the mth detector to be used. The g_m's depict

[3]Note that for construction of the likelihood this is reasonable. However, if one needs to place the templates in the directional space [21], one has to explicitly incorporate the delays in the formalism.

[4]We take $2N$ time samples so that there would be N positive frequency samples as we work in the frequency domain for the rest of the paper.

[5]The Fourier transform is $\tilde{G}(f) = \int_{-\infty}^{\infty} G(t)e^{-2\pi ift}dt$.

[6]$\mathbf{E}[|\tilde{n}_{jm}|^2] = \frac{1}{2}\mathcal{N}_{jm}$, where $\tilde{n}_{jm}$ is the jth frequency component of noise in the mth detector.

[7]The scalar product $\langle\mathbf{a}|\mathbf{b}\rangle_m = 4\Re\sum_{j=1}^{N}\frac{\tilde{a}_j\tilde{b}_j^*}{\mathcal{N}_{jm}} \equiv 4\Re\sum_{j=1}^{N}\tilde{\tilde{a}}_j\tilde{b}_j^*$. $\tilde{\tilde{\mathbf{a}}}$ is the frequency domain vector for the overwhitened signal $\mathbf{a}$.

the scaling in SNR arising solely due to the different noise PSDs. When all the noise PSD's are identical, then $g_m = g$, a constant. Note that this g_m is proportional to the one defined in Ref. [11], Eq. (3.12).

A. Network SNR vector

The form of $\boldsymbol{\rho}^2$ in Eq. (7) motivates us to define an I-dimensional SNR vector $\boldsymbol{\varrho}$ such that $\boldsymbol{\rho}^2 = \boldsymbol{\varrho}^H\boldsymbol{\varrho}$ as below:

$$\boldsymbol{\varrho} \equiv \mathrm{A}_0[\,\mathbf{d} \quad \mathbf{d}^*\,]\begin{bmatrix} \left(\frac{1+\cos\epsilon}{2}\right)^2 e^{-2i\Psi} \\ \left(\frac{1-\cos\epsilon}{2}\right)^2 e^{2i\Psi} \end{bmatrix}. \tag{8}$$

In Eq. (8) the I-dimensional vector $\mathbf{d}$ and its conjugate $\mathbf{d}^*$ characterize the network angular response with respect to the source location and noise weights as below:

$$\mathrm{F}'_m \equiv g_m \mathrm{F}_m = d_m(\theta, \phi, \alpha_m, \beta_m, \gamma_m)e^{-2i\Psi}. \tag{9}$$

Here, components of $\mathbf{F}'$ are the noise weighted complex antenna pattern functions constructed from F_{+m}, $\mathrm{F}_{\times m}$ and g_m. We note that Eq. (8) separates the masses in A_0 and the (ϵ, Ψ) in the two circular polarizations. Further, $\mathbf{d}$ and $\mathbf{d}^*$ together form a two-dimensional complex plane in the I-dimensional complex space. As long as the source and the network is fixed, this plane remains fixed. The network SNR vector $\boldsymbol{\varrho}$ is located in this complex plane.[8]

In general $\mathbf{d}$ and $\mathbf{d}^*$ are not orthogonal to each other; hence, the network SNR square, which is the Euclidean norm square of $\boldsymbol{\varrho}$, will have the cross term between these vectors. Thus, we use SVD technique to express $\boldsymbol{\varrho}$ as sum of two orthogonal vectors, such that the network SNR square $\boldsymbol{\rho}^2$ becomes sum of norm squares of two orthogonal vectors.

The SVD of the matrix $[\,\mathbf{d} \quad \mathbf{d}^*\,]$ is

$$[\,\mathbf{d} \quad \mathbf{d}^*\,] = \underbrace{[\,\hat{\mathbf{u}}_1 \quad \hat{\mathbf{u}}_2\,]}_{\mathbf{U}} \underbrace{\begin{bmatrix} \frac{\|\mathbf{u}_1\|}{\sqrt{2}} & 0 \\ 0 & \frac{\|\mathbf{u}_2\|}{\sqrt{2}} \end{bmatrix}}_{\Sigma} \underbrace{\frac{1}{\sqrt{2}}\begin{bmatrix} e^{i\frac{\delta}{2}} & e^{-i\frac{\delta}{2}} \\ ie^{i\frac{\delta}{2}} & -ie^{-i\frac{\delta}{2}} \end{bmatrix}}_{\mathbf{V}^H}, \tag{10}$$

where $(\mathbf{U}, \Sigma, \mathbf{V})$ have similar form as described in Sec. IV of Ref. [18]. The columns of $\mathbf{U}$, $\hat{\mathbf{u}}_1$, and $\hat{\mathbf{u}}_2$ are the left singular vectors, and those of $\mathbf{V}$ are the right singular vectors of matrix $[\,\mathbf{d} \quad \mathbf{d}^*\,]$. The diagonal elements of Σ are the singular values.

The orthogonal pair $\{\mathbf{u}_1, \mathbf{u}_2\}$ can be written down in terms of the antenna pattern functions as

$$\mathbf{u}_1 \equiv 2\Re[\mathbf{F}'e^{2i\chi}], \qquad \mathbf{u}_2 \equiv 2\Im[\mathbf{F}'e^{2i\chi}], \tag{11}$$

with[9] $\|\mathbf{u}_{1,2}\| = \sqrt{2(\mathbf{d}^H\mathbf{d} \pm |\mathbf{d}^T\mathbf{d}|)}$ and the phase $\chi = \Psi - \frac{\delta}{4}$. Here, $\delta = arg(\mathbf{d}^T\mathbf{d})$ solely depends on the multidetector network orientation with respect to the source location. Thus, for different sky-positions, the χ would vary for a given network configuration.

Substituting back in Eq. (8), we obtain the network SNR vector as a linear combination of two orthogonal vectors

$$\begin{aligned}\boldsymbol{\varrho} = {} & \frac{\mathrm{A}_0}{2}\left(\frac{1+\cos^2\epsilon}{2}\cos 2\chi - i\cos\epsilon\sin 2\chi\right)\mathbf{u}_1 \\ & + \frac{\mathrm{A}_0}{2}\left(\frac{1+\cos^2\epsilon}{2}\sin 2\chi + i\cos\epsilon\cos 2\chi\right)\mathbf{u}_2.\end{aligned} \tag{12}$$

By using the orthogonality property of $\mathbf{u}_1$ and $\mathbf{u}_2$, we can show that $\boldsymbol{\rho}^2$ can be written as the sum of two individual terms arising from the orthogonal vectors in the network SNR vector. Please note that unlike Eq. (7) the above equation is expressed in terms of orthogonal $\{\mathbf{u}_1, \mathbf{u}_2\}$ pair. For the sake of completeness, we give below the coherent network SNR in terms of the individual SNRs:

$$\begin{aligned}\boldsymbol{\rho}^2 = \boldsymbol{\varrho}^H\boldsymbol{\varrho} &= \boldsymbol{\rho}_L^2 + \boldsymbol{\rho}_R^2 \\ &= \frac{\mathrm{A}_0^2\|\mathbf{u}_1\|^2}{4}\underbrace{\left[\left(\frac{1+\cos^2\epsilon}{2}\right)^2\cos^2 2\chi + \cos^2\epsilon\sin^2 2\chi\right]}_{\mathrm{P}_L^2} \\ &\quad + \frac{\mathrm{A}_0^2\|\mathbf{u}_2\|^2}{4}\underbrace{\left[\left(\frac{1+\cos^2\epsilon}{2}\right)^2\sin^2 2\chi + \cos^2\epsilon\cos^2 2\chi\right]}_{\mathrm{P}_R^2}.\end{aligned} \tag{13}$$

In Eq. (12) we can see that the two linear polarizations $(+, \times)$ are linearly combined to form a pair of left (L) and right (R) circular polarizations. More discussion on circular polarizations is given in Sec. IV.

This motivates us to construct two synthetic streams which would each give an individual SNR, $\boldsymbol{\rho}_L$ and $\boldsymbol{\rho}_R$. We address this in the subsequent Sec. IV.

B. Connection to dominant polarization frame

The DP frame is a specific choice of wave frame in which the the real and imaginary parts of the noise weighted complex network antenna pattern vector $\mathbf{F}'^{DP} = \mathbf{F}'^{DP}_+ + i\mathbf{F}'^{DP}_\times$ become orthogonal to each other, i.e.,

$$\sum_{m=1}^{I} \mathrm{F}'^{DP}_{+m}\mathrm{F}'^{DP}_{\times m} = 0. \tag{14}$$

[8]The vector $\mathbf{d}$ is the noise weighted version of the one defined in Ref. [18]. The complex plane formed by $\mathbf{d}$ and $\mathbf{d}^*$ is called the "polarization plane" or "helicity plane" in the literature. For further details, see Refs. [11,18].

[9]$\|.\|$ represents the Euclidean norm of a vector.

In Eq. (9), it is apparent that the Ψ dependence in the complex antenna pattern is in the phase. This ensures freedom in the choice of Ψ *via* the orientation of the wave frame with respect the reference frame. If we rotate the wave plane by an additional angle $\Delta\Psi$ about the line of sight (Z axis), the network antenna pattern for this newly rotated wave frame can be obtained by applying an equivalent transformation on $\mathbf{F}$ as $\mathbf{F}\exp(-2i\Delta\Psi)$. That would also transform the signal as $\mathbf{h}\exp(-2i\Delta\Psi)$ keeping the response Eq. (3) invariant. This freedom in the choice of Ψ is explored to obtain the DP frame. In other words, the DP frame is obtained by a certain choice of polarization angle Ψ^{DP} of the wave frame with respect to the geocentric frame such that it will satisfy the condition given in Eq. (14). The phrase "dominant polarization frame" was coined in the context of the detection of bursts by Klimenko *et al.* [16] and recently in the inspiral search with multi-detector network in Ref. [13].

Thus, the noise weighted complex network antenna pattern vector in DP frame can be written as

$$\mathbf{F}'^{DP} = \mathbf{d}e^{-2i\Psi^{DP}}. \tag{15}$$

However, from Eq. (11) we note that the vector $\mathbf{F}'e^{2i\chi}$ has orthogonal real and imaginary component vectors, which is precisely the condition for antenna pattern vectors in the DP frame. Thus, the SVD provides a natural connection to the DP frame through its construction, where the singular values are in descending order.

In summary,

$$\begin{aligned}\mathbf{F}'^{DP} &= \mathbf{F}'e^{2i\chi} = \frac{\mathbf{u}_1 + i\mathbf{u}_2}{2} = \mathbf{d}e^{-i\frac{\delta}{2}},\\ \mathbf{F}'^{DP}_{+} &= \frac{\mathbf{u}_1}{2} \quad \text{and} \quad \mathbf{F}'^{DP}_{\times} = \frac{\mathbf{u}_2}{2},\end{aligned} \tag{16}$$

and $\Psi^{DP} = \delta/4$. The DP frame is obtained by rotating the wave frame about the z axis by an angle $\chi = \Psi - \delta/4$ in the clockwise direction. The DP frame pertains to the source; i.e., if one changes the source location, the $\mathbf{d}$-$\mathbf{d}^*$ plane will be different. The χ will change via δ. Further when the source location remains the same but the polarization angle Ψ changes, then also χ changes via Ψ.

IV. APERTURE SYNTHESIS IN GW INSPIRAL SEARCH

As mentioned earlier, more than one detector is necessary to determine GW polarization as well as the localization of the sources [24]. In the following discussion, we construct two effective synthetic data streams out of I detector data streams in the network; they together carry the full network SNR as given in Eq. (7). Since GWs carry two polarizations in the Einsteinian gravity, the signal resides in the two-dimensional subspace of I-dimensional network space, and hence only two independent data streams are sufficient to provide information about the polarization in the network formalism. We show that the constructed data streams provide that information. In the past [11,13,18], the synthetic data streams were shown to be the byproduct of maximizing the network LLR over the four extrinsic parameters $(A, \phi_a, \epsilon, \Psi)$. However, here in this section, we show that the synthetic streams can be constructed prior to the MLR analysis. This is similar to the spirit of aperture synthesis technique in the electromagnetic window such as optical or radio used in very large telescope interferometer [25] or very long baseline interferometry [26], where an effective antenna is constructed out of a linear combination of data from different telescopes.

Below, we construct the synthetic data streams using $\mathbf{u}_1$ and $\mathbf{u}_2$ and show that they individually give the matched filter SNR equal to $\boldsymbol{\rho}_L$ and $\boldsymbol{\rho}_R$.

A. Signal $\mathbf{s}_m$ in the DP frame

In the rest of the paper, we work in the new frame provided by the SVD, also known as the DP frame. We rewrite the antenna pattern $\mathbf{F}$ in terms of $\mathbf{u}_1$ and $\mathbf{u}_2$ and then express the network signal as below.

Using Eqs. (3) and (16), the time domain signal vector at the mth detector is

$$\begin{aligned}\mathbf{s}_m &= \frac{1}{2}\Re\left[\mathbf{h}e^{2i\chi}\frac{u_{1m}}{g_m}\right] + \frac{1}{2}\Im\left[\mathbf{h}e^{2i\chi}\frac{u_{2m}}{g_m}\right],\\ &= \Re\left[\mathbf{h}e^{2i\chi}\left(\frac{u_{1m} + iu_{2m}}{2g_m}\right)^*\right] \equiv \Re[\mathbf{h}^{DP}\mathbf{F}^{DP*}_m],\end{aligned} \tag{17}$$

where $\mathbf{h}^{DP} = \mathbf{h}\exp(2i\chi)$ and $\mathbf{F}^{DP} = \mathbf{F}\exp(2i\chi)$ are the complex GWs as well as the network antenna pattern function in the DP frame, respectively.

From Eqs. (4) and (16), the jth frequency component of the frequency domain signal in the mth detector $[\tilde{\mathbf{s}}_m]_j = \tilde{\mathcal{S}}_{jm}$ can be expressed in terms of the linear combination of $\mathbf{F}^{DP}_{+,\times}$ in the DP frame. Further, the amplitude A_0, initial phase ϕ_a, and frequency dependent part, namely, $\tilde{\mathbf{h}}_0$, are factored out as shown below:

$$\begin{aligned}\tilde{\mathcal{S}}_{jm} &= \mathrm{A}_0 e^{i\phi_a}\tilde{h}_{0j}\left[\left(\frac{1+\cos^2\epsilon}{2}\cos 2\chi + i\cos\epsilon\sin 2\chi\right)\mathrm{F}^{DP}_{+m}\right.\\ &\quad \left. + \left(\frac{1+\cos^2\epsilon}{2}\sin 2\chi - i\cos\epsilon\cos 2\chi\right)\mathrm{F}^{DP}_{\times m}\right]\\ &\equiv \mathrm{A}_0\tilde{h}_{0j}[\mathrm{P}_L\mathrm{F}^{DP}_{+m}e^{i\Phi_L} + \mathrm{P}_R\mathrm{F}^{DP}_{\times m}e^{i\Phi_R}].\end{aligned} \tag{18}$$

The $\mathrm{P}_{L,R}$ are the polarization amplitudes in the DP frame as defined in Eq. (13). This carries the effect of rotation by 2χ of the signal which mixes the two linear GW polarizations into a pair of *L and R circular polarizations*. The polarization phases are

$$\Phi_L(\epsilon,\chi) = \tan^{-1}\left[\tan(2\chi)\frac{2\cos\epsilon}{1+\cos^2\epsilon}\right] + \phi_a, \quad (19)$$

$$\Phi_R(\epsilon,\chi) = \Phi_L\left(\epsilon,\chi+\frac{\pi}{4}\right). \quad (20)$$

As expected the Φ_R phase is obtained by rotating χ by $\pi/4$ in Φ_L, the property of GW polarization pairs. The above polarization terms, namely, $\{P_{L,R}e^{i\Phi_{L,R}}\}$, can be shown to be equal to

$$P_L e^{i\Phi_L} = [T^*_{2+2}(\chi,\epsilon,0) + T^*_{2-2}(\chi,\epsilon,0)] \quad (21)$$

$$P_R e^{i\Phi_R} = i[T^*_{2-2}(\chi,\epsilon,0) - T^*_{2+2}(\chi,\epsilon,0)], \quad (22)$$

respectively, which describe the circular polarizations expressed in terms of rank-2 Gel–Fand function T_{mn} [27].[10]

In the next subsection, we use this separation feature of the signal to construct the synthetic streams.

B. Network matched filter

In this section, we introduce the notion of a matched filter designed for a the multidetector analysis which not only combines the spectral but also the network features. We call this filter as the network matched filter.

Let the frequency domain delayed network data stream be given by $\tilde{\boldsymbol{\mathcal{X}}} = [\tilde{\mathbf{x}}_1\tilde{\mathbf{x}}_2\ldots\tilde{\mathbf{x}}_I]$ with $\tilde{\mathbf{x}}_m = \tilde{\mathbf{s}}_m + \tilde{\mathbf{n}}_m$ and $\tilde{\mathbf{n}}_m$ be the frequency domain noise vector corresponding to mth detector. To proceed further, we make the following constructs:

(1) Overwhitened data stream: Construct the overwhitened data stream incorporating the noise PSD of the individual antennas denoted by $\tilde{\tilde{\mathcal{X}}}_{jm} = \frac{\tilde{\mathcal{X}}_{jm}}{\mathcal{N}_{jm}}$.

(2) Synthetic data stream: The overwhitened synthetic data stream $\tilde{\tilde{\mathbf{z}}}$ is constructed from the linear combination of individual overwhitened data streams as

$$\tilde{\tilde{z}}_j \equiv \sum_{m=1}^{I} \alpha_m \tilde{\tilde{\mathcal{X}}}_{jm}, \quad (23)$$

with real linear coefficients α_m. The overwhitened data are used for the synthetic data stream construction in order to incorporate the individual noise PSDs.

We show in the rest of the section that using the classical idea of matched filtering, we can tune α_m such that the resulting synthetic data stream would extract either L or R circular polarization.

In the next subsection, we remind the reader that the classical derivation of the matched filter used for the single detector context.

1. Single detector matched filter

If $\tilde{\mathbf{k}}$ is a filter, then the filtered output of $\tilde{\mathbf{z}}$ through this filter is $\langle\mathbf{z}|\mathbf{k}\rangle$. Here (in order to avoid the excess notations) for this subsubsection, let us assume that $\tilde{\mathbf{z}}$ denotes the unwhitened data of the single detector.

The SNR of the filtered output is [28]

$$\mathrm{SNR} = \frac{\mathbf{E}[\langle\mathbf{z}|\mathbf{k}\rangle]}{\boldsymbol{\sigma}[\langle\mathbf{z}|\mathbf{k}\rangle]|_{\tilde{s}=0}} = \frac{4\Re[\sum_{j=1}^{N}\mathbf{E}(\tilde{\tilde{z}}_j\tilde{k}^*_j)]}{\sqrt{\mathrm{E}[(4\Re[\sum_{l=1}^{N}\tilde{\tilde{z}}_l\tilde{k}^*_l])^2]|_{\tilde{s}=0}}}, \quad (24)$$

where $\mathbf{E}[.]$ represents the expectation and $\boldsymbol{\sigma}[.]$ represents the standard deviation. The single detector SNR further simplifies to

$$\text{Single detector SNR} = \frac{4\Re[\sum_{j=1}^{N}\tilde{\tilde{s}}_j\tilde{k}^*_j]}{\sqrt{4\sum_{j=1}^{N}\frac{|\tilde{k}_j|^2}{\mathcal{N}_j}}} = \langle\mathbf{s}|\hat{\mathbf{k}}\rangle. \quad (25)$$

Here $\mathcal{N}_j$ is the jth frequency component of one sided noise power spectral density vector.

The filter norm is $\sqrt{\langle\mathbf{k}|\mathbf{k}\rangle}$. As is known, the above SNR would be optimal when the filter vector is aligned to the signal vector, i.e., $\tilde{k}_j \propto \tilde{s}_j$, known as the matched filter.

Now, let us explore these ideas in the context of the multidetector scenario.

2. Network matched filter

The matched filter is that filter which gives the optimum SNR in Gaussian noise. However, the signal in DP frame is separated in such a way that the noise weighted antenna patterns are orthogonal. Let us apply the matched filter notion with the aim that the resultant combined spectral as well as network filter *via* α_m would capture the individual polarizations. We show below that in this exercise, this amounts to constructing a combined spectral-network matched filter.

Consider Eq. (24) with $\tilde{\mathbf{z}}$ as the synthetic stream defined in Eq. (23). Then, Eq. (24) can be simplified to

$$\mathrm{SNR} = \frac{4\Re[\sum_{j=1}^{N}\sum_{m=1}^{I}\tilde{\tilde{\mathcal{S}}}_{jm}\tilde{\mathcal{K}}^*_{jm}]}{\sqrt{4\sum_{j=1}^{N}\sum_{m=1}^{I}\frac{|\tilde{\mathcal{K}}_{jm}|^2}{\mathcal{N}_{jm}}}}, \quad (26)$$

where the matrix $\tilde{\boldsymbol{\mathcal{K}}} = \tilde{\mathbf{k}}\otimes\boldsymbol{\alpha}$, i.e., $\tilde{\mathcal{K}}_{jm} = \tilde{k}_j\alpha_m$, and the mth column vector $\tilde{\mathcal{K}}_m = \alpha_m\tilde{\mathbf{k}}$.

[10]The rank-2 Gel–Fand functions

$$T^2_{2\pm2}(\chi,\epsilon,0) = \frac{(1\pm\cos\epsilon)^2}{4}\exp(\mp2i\chi).$$

Since throughout the paper we use only rank-2 Gel–Fand functions, we drop the superscript 2 from T^2_{mn}.

Further, the denominator of Eq. (26),

$$\sqrt{4\sum_{j=1}^{N}\sum_{m=1}^{I}\frac{|\tilde{\mathcal{K}}_{jm}|^2}{\mathcal{N}_{jm}}}=\sqrt{\sum_{m=1}^{I}\alpha_m^2\langle\mathbf{k}|\mathbf{k}\rangle_m}, \tag{27}$$

is the Frobeinus matrix norm of $\tilde{\mathcal{K}}_{\mathbf{N}\times\mathbf{I}}$ in the combined spectral-network $(N\times I)$ space defined as $\|\tilde{\mathcal{K}}\|^2\equiv \mathrm{Tr}(\langle\tilde{\mathcal{K}}_m,\tilde{\mathcal{K}}_n\rangle)$, which is same as the right-hand side of Eq. (27). The subscript m in $\langle\mathbf{k}|\mathbf{k}\rangle_m$ denotes the noise PSD is that of mth detector.

It is interesting to note that Eq. (26) has the same structure of a conventional single detector matched filter SNR in Eq. (25). For a single detector, the filter is a one-dimensional vector in the spectral direction. As the matched filter is that filter which gives the maximum SNR, which should be aligned along the signal, i.e., $\tilde{k}_j\propto\tilde{s}_j$ for the single detector case.

While in the multidetector case, $\tilde{\mathcal{K}}$ is a two-dimensional $(N\times I)$ combined spectral network filter. Since $\tilde{\boldsymbol{\mathcal{S}}}$ can be decomposed into frequency and network components, the optimal combined filter should *match* with $\tilde{\boldsymbol{\mathcal{S}}}$ (or part of $\tilde{\boldsymbol{\mathcal{S}}}$) in the same spirit as that of the single detector case described above. Owing to the facts that were detailed in Eq. (18), we recall that the network signal has two constituent parts. Here, we construct that filter which captures either of the two circular polarizations as shown below:

(1) $\tilde{\mathcal{K}}_L$: *Network matched filter for left circular polarization:* To capture the plus polarization of the DP frame (left circular polarization) in Eq. (18), $\tilde{\mathcal{K}}_L$ should be aligned to the *Left* polarization part of the $\tilde{\boldsymbol{\mathcal{S}}}$, which we call $\tilde{\mathcal{K}}_L\equiv\tilde{\mathbf{k}}_L\otimes\boldsymbol{\alpha}_L$. The alignment condition demands that it should satisfy

$$\tilde{k}_{Lj}\propto\tilde{h}_{0j}e^{i\Phi_L}\quad\text{and}\quad\alpha_{Lm}\propto \mathrm{F}^{DP}_{+m} \tag{28}$$

together. Since the Frobeinus *norm* of $\tilde{\mathcal{K}}_L$ is $\|\mathbf{F}'^{DP}_{+}\|$, the components of the normalized network plus filter $\tilde{\mathcal{K}}_L$ become

$$\tilde{k}_{Lj}=\tilde{h}_{0j}e^{i\Phi_L},\qquad \alpha_{Lm}=\frac{\mathrm{F}^{DP}_{+m}}{\|\mathbf{F}'^{DP}_{+}\|}. \tag{29}$$

Using Eqs. (26) and (29), the corresponding SNR becomes

$$4\Re\left[\sum_{j=1}^{N}\sum_{m=1}^{I}\tilde{\tilde{\mathcal{S}}}_{jm}\tilde{\mathcal{K}}_{Ljm}\right]=\boldsymbol{\rho}_L. \tag{30}$$

(2) $\tilde{\mathcal{K}}_R$: *Network matched filter for right circular polarization:* To capture the cross polarization of the DP frame (right circular polarization) in Eq. (18), we construct another filter, $\tilde{\mathcal{K}}_R\equiv\tilde{\mathbf{k}}_R\otimes\boldsymbol{\alpha}_R$, such that together it should satisfy

$$\tilde{k}_{Rj}\propto\tilde{h}_{0j}e^{i\Phi_R}\quad\text{and}\quad\alpha_{Rm}\propto \mathrm{F}^{DP}_{\times m}. \tag{31}$$

The Frobeinus norm of $\tilde{\mathcal{K}}_R$ is $\|\mathbf{F}'^{DP}_{\times}\|$ gives the components of normalized network cross filter $\tilde{\mathcal{K}}_R$,

$$\tilde{k}_{Rj}=\tilde{h}_{0j}e^{i\Phi_R},\qquad \alpha_{Rm}=\frac{\mathrm{F}^{DP}_{\times m}}{\|\mathbf{F}'^{DP}_{\times}\|}, \tag{32}$$

with the corresponding SNR as given by

$$4\Re\left[\sum_{j=1}^{N}\sum_{m=1}^{I}\tilde{\tilde{\mathcal{S}}}_{jm}\tilde{\mathcal{K}}_{Rjm}\right]=\boldsymbol{\rho}_R. \tag{33}$$

In summary, the synthetic streams constructed from the overwhitened data streams which capture the individual polarizations in the DP frame are

$$\tilde{\tilde{\mathbf{z}}}_L=\sum_{m=1}^{I}\frac{\mathrm{F}^{DP}_{+m}}{\|\mathbf{F}'^{DP}_{+}\|}\tilde{\tilde{X}}_{jm},\qquad \tilde{\tilde{\mathbf{z}}}_R=\sum_{m=1}^{I}\frac{\mathrm{F}^{DP}_{\times m}}{\|\mathbf{F}'^{DP}_{\times}\|}\tilde{\tilde{X}}_{jm}. \tag{34}$$

They together give the total network SNR as the sum squares of individual SNRs. The total signal power in the individual detectors of the network is now distributed among the synthetic streams $\tilde{\mathbf{z}}_L$ and $\tilde{\mathbf{z}}_R$, which when processed with filters $\tilde{\mathbf{k}}_L$ and $\tilde{\mathbf{k}}_R$ independently captures the two polarizations in the DP frame. By using Eqs. (29), (30), (32), and (33), we can write the respective SNRs as

$$\boldsymbol{\rho}_L=\langle\mathbf{z}_L|\mathbf{k}_L\rangle|_{\mathbf{n}=0},\qquad \boldsymbol{\rho}_R=\langle\mathbf{z}_R|\mathbf{k}_R\rangle|_{\mathbf{n}=0}. \tag{35}$$

Thus, we have shown that extending the concept of the matched filter to the network gives us two effective synthetic data streams which can be further processed.

C. Special case: Same noise for all detectors

In this subsection, we consider an idealistic situation where all the detectors have same noise PSD, i.e., g_m becomes equal to a constant g for all detectors. Then from Eq. (34), we can see that the "noise free" synthetic streams $\tilde{\mathbf{z}}^s_{L,R}$ are nothing but the projections of the network signal matrix $\tilde{\boldsymbol{\mathcal{S}}}$ on the orthonormal vectors $\hat{\mathbf{F}}^{DP}_{+,\times}$ with an overall weight $1/g$. If we expand $\tilde{\boldsymbol{\mathcal{S}}}$ as in Eq. (18), we can further simplify $\tilde{\mathbf{z}}^s_{L,R}$ into a linear combination of GW polarizations $\tilde{\mathbf{h}}_{+,\times}$ similar to a pair of ordinary interferometric detector signals as shown below:

$$\begin{aligned}\tilde{\mathbf{z}}^s_L&=\frac{\|\mathbf{F}^{DP}_{+}\|}{g}(\tilde{\mathbf{h}}_+\cos 2\chi-\tilde{\mathbf{h}}_\times\sin 2\chi),\\ \tilde{\mathbf{z}}^s_R&=\frac{\|\mathbf{F}^{DP}_{\times}\|}{g}(\tilde{\mathbf{h}}_+\sin 2\chi+\tilde{\mathbf{h}}_\times\cos 2\chi).\end{aligned} \tag{36}$$

Please note the equivalent antenna pattern of $\tilde{\mathbf{z}}^s_R$ is $\pi/4$ out of phase with that of $\tilde{\mathbf{z}}^s_L$.

V. MULTIDETECTOR MAXIMUM LIKELIHOOD RATIO AND NETWORK SYNTHETIC STREAMS

In this section, we carry out MLR analysis for the inspiral detection with a multidetector network. This has been already done in the literatures [11,13,18] in different contexts as well as notations. Here, we construct MLR statistic in a much more straightforward way. We further compare this work with the previous works and thus bring all earlier multidetector inspiral related search formalisms under the same notations.

In the multidetector network MLR detection technique, the network LLR is maximized over signal parameters, and a test statistic is obtained, which is then compared with the threshold for the detection. For high SNR cases, the MLR technique is known to be optimal.

A. Network likelihood ratio

Assuming the Gaussian, additive noise in each detector data, the LLR for a multidetector network with I constituent detectors is the sum of LLRs of individual antennas and is given by [13]

$$\Lambda = \sum_{m=1}^{I} \langle \mathbf{x}_m | \mathbf{s}_m \rangle - \frac{1}{2} \langle \mathbf{s}_m | \mathbf{s}_m \rangle. \tag{37}$$

Rearranging terms and a little algebra as given in Appendix A, we can reexpress the above equation in terms of the synthetic data streams as

$$2\Lambda = [2\boldsymbol{\rho_L} \langle \mathbf{z}_L | \mathbf{h}_0 e^{i\Phi_L} \rangle - \boldsymbol{\rho_L^2}] + [2\boldsymbol{\rho_R} \langle \mathbf{z}_R | \mathbf{h}_0 e^{i\Phi_R} \rangle - \boldsymbol{\rho_R^2}]. \tag{38}$$

We note that Eq. (38) can be viewed as the sum of the LLRs of two independent synthetic detectors, where $\Phi_{L,R}$ carries the constant phase which incorporates the initial phase plus the polarization angles and $\boldsymbol{\rho}_{L,R}$ are the SNRs of the two synthetic data streams.

We note that, in terms of synthetic streams, the four extrinsic parameters $(\mathrm{A}_0, \phi_a, \epsilon, \Psi)$ are now mapped in to a set of two effective SNRs and two effective phases, namely, $(\boldsymbol{\rho}_L, \boldsymbol{\rho}_R, \Phi_L, \Phi_R)$.

B. Maximization of network LLR

Now we maximize Λ over the new extrinsic parameters $(\boldsymbol{\rho}_L, \boldsymbol{\rho}_R, \Phi_L, \Phi_R)$ to obtain the maximum log likelihood ratio, $\hat{\Lambda}$ [11,13,18]. The new extrinsic parameters give the reparametrized physical parameters $(\mathrm{A}_0, \phi_a, \epsilon, \Psi)$ where the relation between them is summarized in Appendix B. Below, we maximize Λ over the new set; first over the amplitudes and then over the phase, respectively:

(1) Amplitude maximization: Maximization over $\boldsymbol{\rho}_{L,R}$ is the same as that in the case of a single detector [7], and it results in

$$2\hat{\Lambda}|_{\boldsymbol{\rho}_L, \boldsymbol{\rho}_R} = \langle \mathbf{z}_L | \mathbf{h}_0 e^{i\Phi_L} \rangle^2 + \langle \mathbf{z}_R | \mathbf{h}_0 e^{i\Phi_R} \rangle^2, \tag{39}$$

and the MLR amplitude estimates become

$$\hat{\boldsymbol{\rho}}_L = \langle \mathbf{z}_L | \mathbf{h}_0 e^{i\Phi_L} \rangle, \qquad \hat{\boldsymbol{\rho}}_R = \langle \mathbf{z}_R | \mathbf{h}_0 e^{i\Phi_R} \rangle. \tag{40}$$

(2) Phase maximization: Since Φ_L and Φ_R are independent, maximization of LLR over them amounts to individually maximizing each term of the sum in Eq. (39). Thus, the maximum likelihood estimates of $\Phi_{L,R}$ are

$$\hat{\Phi}_L = \arg\left[\sum_{j=1}^{N} \tilde{\tilde{z}}_{L,j} \tilde{h}_{0j}^*\right], \qquad \hat{\Phi}_R = \arg\left[\sum_{j=1}^{N} \tilde{\tilde{z}}_{R,j} \tilde{h}_{0j}^*\right]. \tag{41}$$

In summary,

$$2\hat{\Lambda} = 16\left[\left|\sum_{j=1}^{N} \tilde{\tilde{z}}_{L,j} \tilde{h}_{0j}^*\right|^2 + \left|\sum_{j=1}^{N} \tilde{\tilde{z}}_{R,j} \tilde{h}_{0j}^*\right|^2\right]. \tag{42}$$

We write one individual term in Eq. (42) as follows:

$$\begin{aligned} &\left|\sum_{j=1}^{N} \tilde{\tilde{z}}_{L,Rj} \tilde{h}_{0j}^*\right|^2 \\ &= \left(\Re\left[\sum_{j=1}^{N} \tilde{\tilde{z}}_{L,Rj} \tilde{h}_{0j}^*\right]\right)^2 + \left(\Re\left[\sum_{j=1}^{N} \tilde{\tilde{z}}_{L,Rj} \tilde{h}_{\pi/2j}^*\right]\right)^2. \\ &= \frac{\langle \mathbf{z}_{L,R} | \mathbf{h}_0 \rangle^2 + \langle \mathbf{z}_{L,R} | \mathbf{h}_{\pi/2} \rangle^2}{16}. \end{aligned} \tag{43}$$

Thus, the MLR simplifies to

$$2\hat{\Lambda} = \langle \mathbf{z}_L | \mathbf{h}_0 \rangle^2 + \langle \mathbf{z}_L | \mathbf{h}_{\pi/2} \rangle^2 + \langle \mathbf{z}_R | \mathbf{h}_0 \rangle^2 + \langle \mathbf{z}_R | \mathbf{h}_{\pi/2} \rangle^2. \tag{44}$$

This can be described as a quadrature sum of powers in synthetic streams $\tilde{\mathbf{z}}_L$ and $\tilde{\mathbf{z}}_R$. This is similar to the single detector statistic which contains the quadrature sum of powers in a single detector data stream. From Eqs. (35) and (42), we can see under no noise condition [11,13,18]

$$2\hat{\Lambda} = \boldsymbol{\rho_L}^2 + \boldsymbol{\rho_R}^2. \tag{45}$$

VI. CONNECTION TO THE EXISTING LITERATURE

In the GW multidetector inspiral search, network MLR statistics maximized over four extrinsic parameters has been formalized in the literature [11,13]. Though the problem is same, the parametrization depends on the way the problem is cast. However, the final network MLR maximized over the extrinsic parameters is the same.

In this section, we carry out a comparison between various formalisms under the same notations as given here, which till now has not been done in the literature so far.

A. Synthetic streams and Harry–Fairhurst [13] approach

In Ref. [13], the authors cast the multidetector MLR problem into the $\mathcal{F}$ statistic. The polarizations were written down in terms of the linear combination of the four amplitudes on which the extrinsic parameters are mapped, i.e.,

$$(A_0, \phi_a, \epsilon, \Psi) \Rightarrow (\mathcal{A}_1, \mathcal{A}_2, \mathcal{A}_3, \mathcal{A}_4). \tag{46}$$

For explicit relations, please visit Appendix B. Later the maximum likelihood analysis is carried out in DP frame, where $2\hat{\Lambda}$ is simplified to quadrature sum of powers in $+$ and $\times$ polarizations. Here, the maximization of network LLR over the four amplitudes is performed in a single step.

Below, we derive the multidetector MLR of Ref. [13], Eq. (2.33), starting from the notations in this paper.

In Eq. (39),

$$\begin{aligned}\langle \mathbf{z}_{L,R}|\mathbf{h}_0\rangle &= \frac{4}{\|\mathbf{F}'^{DP}_{+,\times}\|}\Re\left[\sum_{j=1}^{N}\sum_{m=1}^{I}\tilde{\tilde{X}}_{jm}h_{0j}^{*}\mathrm{F}^{DP}_{+,\times m}\right]\\ &= \frac{1}{\|\mathbf{F}'^{DP}_{+,\times}\|}\sum_{m=1}^{I}\langle \mathbf{x}_m|\mathbf{h}_0\mathrm{F}^{DP}_{+,\times m}\rangle,\\ \text{and}\quad \langle \mathbf{z}_{L,R}|\mathbf{h}_{\pi/2}\rangle &= \frac{1}{\|\mathbf{F}'^{DP}_{+,\times}\|}\sum_{m=1}^{I}\langle \mathbf{x}_m|\mathbf{h}_{\pi/2}\mathrm{F}^{DP}_{+,\times m}\rangle.\end{aligned} \tag{47}$$

Further,

$$\|\mathbf{F}'^{DP}_{+,\times}\|^2 = \sum_{m=1}^{I} g_m^2\mathrm{F}^2_{+,\times m} = \sum_{m=1}^{I}\langle \mathbf{h}_0\mathrm{F}_{+,\times m}|\mathbf{h}_0\mathrm{F}_{+,\times m}\rangle.$$

Now substituting back in Eq. (44),

$$\begin{aligned}2\hat{\Lambda} = &\frac{[\sum_m\langle \mathbf{x}_m|\mathbf{h}_0\mathrm{F}^{DP}_{+m}\rangle]^2 + [\sum_m\langle \mathbf{x}_m|\mathbf{h}_{\pi/2}\mathrm{F}^{DP}_{+m}\rangle]^2}{\sum_m\langle \mathbf{h}_0\mathrm{F}_{+m}|\mathbf{h}_0\mathrm{F}_{+m}\rangle}\\ &+\frac{[\sum_m\langle \mathbf{x}_m|\mathbf{h}_0\mathrm{F}^{DP}_{\times m}\rangle]^2 + [\sum_m\langle \mathbf{x}_m|\mathbf{h}_{\pi/2}\mathrm{F}^{DP}_{\times m}\rangle]^2}{\sum_m\langle \mathbf{h}_0\mathrm{F}_{\times m}|\mathbf{h}_0\mathrm{F}_{\times m}\rangle}.\end{aligned} \tag{48}$$

Absorbing the summation over m following the definition Eq. (2.21) of Ref. [13], Eq. (48) becomes Eq. (2.33) of Ref. [13].[11] Also one can show that $\tilde{\tilde{\mathbf{z}}}_{L,R}$ are related to overwhitened synthetic streams $o_{+,\times}$ defined in Eq. (2.35) of Ref. [13] as follows:

$$o_{+,\times} = \|\mathbf{F}'^{DP}_{+,\times}\|\tilde{\tilde{\mathbf{z}}}_{L,R}. \tag{49}$$

[11] $\langle \mathbf{a}|\mathbf{b}\rangle$ is same as $(\mathbf{a}|\mathbf{b})$ defined in Eq. (2.17) of Ref. [13].

The two pairs of synthetic streams differ by constants, which is different for both the synthetic streams. The final maximized multidetector LLR matches Eq. (44) as expected.

B. Synthetic streams and Pai *et al.* [11] approach

In Ref. [11], the multidetector coherent statistic was obtained by successive maximization of amplitude A_0, initial phase ϕ_a similar to the single detector statistic. The polarization angles (ϵ, ψ) are maximized at a time using the symmetry properties of the rotation group and Gel–Fand functions. The maximized network LLR thus obtained contains the sum square of four terms as is shown in Eq. (4.11) of Ref. [11] similar to Eq. (2.33) of Ref. [13] and Eq. (44) above. We explicitly give the Eq. (4.11) of Ref. [11],

$$\begin{aligned}2\hat{\Lambda} &= |\hat{\mathsf{v}}^{+}\cdot\mathsf{C}|^2 + |\hat{\mathsf{v}}^{-}\cdot\mathsf{C}|^2\\ &= (c_0^{+})^2 + (c_{\pi/2}^{+})^2 + (c_0^{-})^2 + (c_{\pi/2}^{-})^2\end{aligned} \tag{50}$$

where the elements of I-dimensional complex vector C,

$$C^m = c_0^m + ic_{\pi/2}^m, \tag{51}$$

combine the correlations of the two quadratures of the normalized template with the data with $c_0^m = \frac{1}{g_m}\langle \mathbf{h}_0|\mathbf{x}_m\rangle_m$ and $c_{\pi/2}^m = \frac{1}{g_m}\langle \mathbf{h}_{\pi/2}|\mathbf{x}_m\rangle_m$. Further,

$$\hat{\mathsf{v}}^{\pm} = \frac{\mathsf{v}^{\pm}}{\|\mathsf{v}^{\pm}\|} = \frac{\widehat{\Re(\mathbf{d})} \pm \widehat{\Im(\mathbf{d})}}{\|(\widehat{\Re(\mathbf{d})} \pm \widehat{\Im(\mathbf{d})})\|} \tag{52}$$

is a pair of real unit vectors which span the two-dimensional polarization plane in the I-dimensional space. Thus, if we take a representative individual term in Eq. (50), it becomes

$$(c_0^{+})^2 = \left(\sum_{m=1}^{I}\frac{\mathsf{v}_m^{+}}{g_m\|\mathsf{v}^{+}\|}\langle \mathbf{x}_m, \mathbf{h}_0\rangle_m\right)^2 \equiv \langle \mathbf{z}_{+}|\mathbf{h}_0\rangle^2. \tag{53}$$

Thus, based on Eq. (53), the corresponding synthetic streams are

$$\tilde{\tilde{\mathbf{z}}}_{+j} \equiv \sum_{m=1}^{I}\frac{\mathsf{v}_m^{+}}{g_m\|\mathsf{v}^{+}\|}\tilde{\tilde{X}}_{jm}, \qquad \tilde{\tilde{\mathbf{z}}}_{-j} \equiv \sum_{m=1}^{I}\frac{\mathsf{v}_m^{-}}{g_m\|\mathsf{v}^{-}\|}\tilde{\tilde{X}}_{jm}, \tag{54}$$

which give the SNR's ρ_{+} and ρ_{-} such that in the no noise case

$$2\hat{\Lambda} = \rho_{+}^2 + \rho_{-}^2. \tag{55}$$

C. SNRs in two pairs of synthetic data streams

In the previous sections, we show that the network SNR square can be split into the sum of squares of SNRs of two

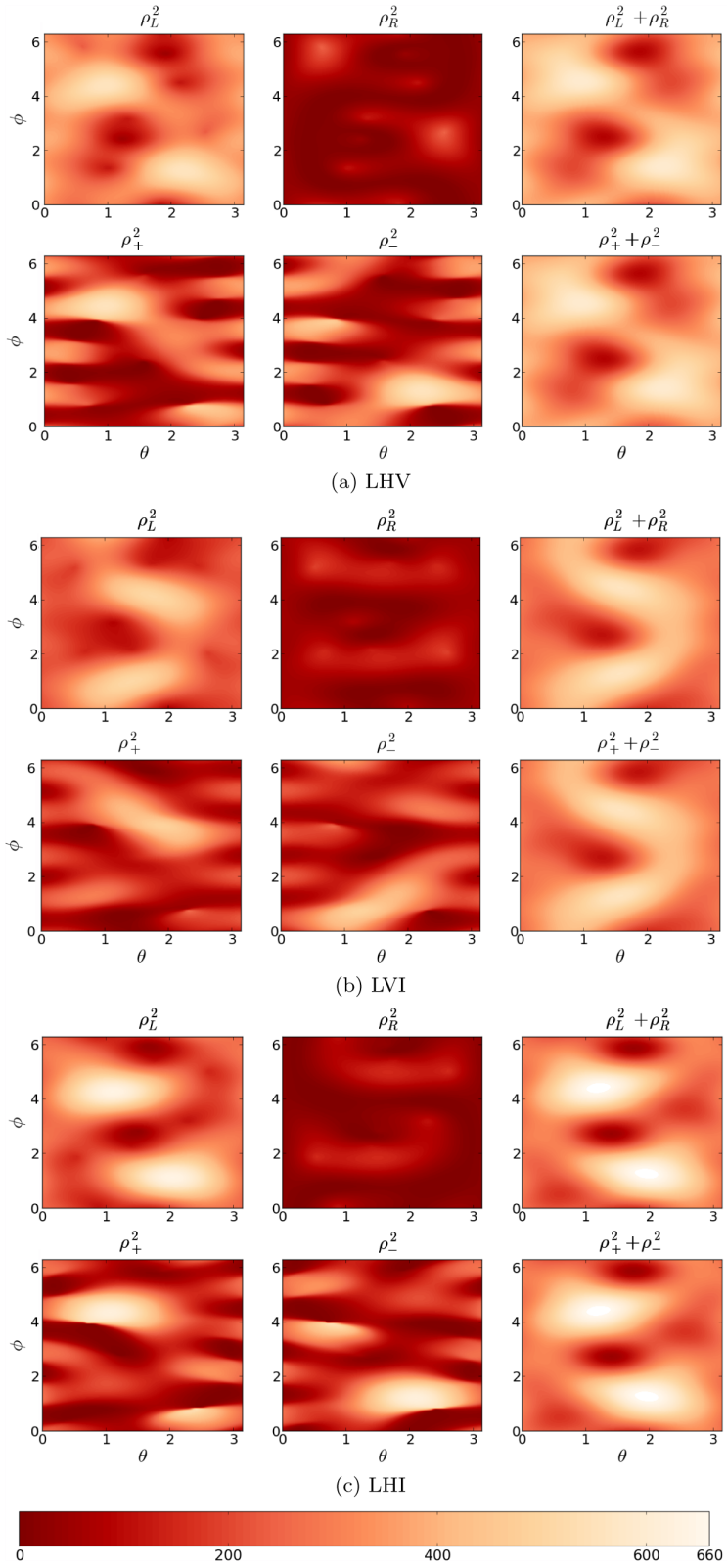

(a) LHV

(b) LVI

(c) LHI

FIG. 1 (color online). Directional SNR squares $\boldsymbol{\rho_L^2}$, $\boldsymbol{\rho_R^2}$, $\boldsymbol{\rho_+^2}$, $\boldsymbol{\rho_-^2}$, and $\boldsymbol{\rho^2}_{\text{net}}$ for various three network configurations with m_1, $m_2 = 1.4$, $\epsilon = \pi/4$, $\Psi = \pi/4$, and $r = 150$ Mpc. with the same noise spectral densities for all detectors.

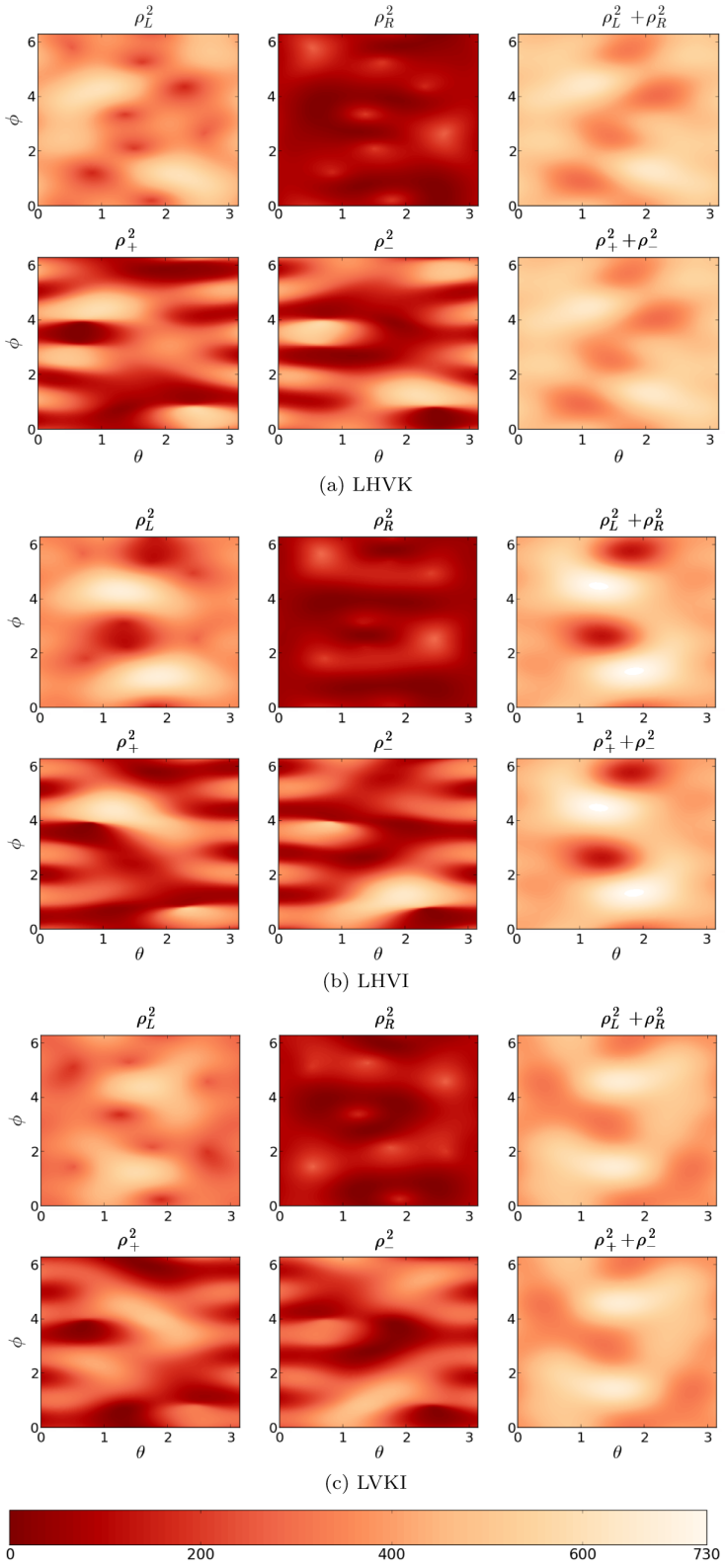

(a) LHVK

(b) LHVI

(c) LVKI

FIG. 2 (color online). Directional SNR Squares $\boldsymbol{\rho_L^2}$, $\boldsymbol{\rho_R^2}$, $\boldsymbol{\rho_+^2}$, $\boldsymbol{\rho_-^2}$, and $\boldsymbol{\rho^2}_{\text{net}}$ for various four detector network configurations with m_1, $m_2 = 1.4$, $\epsilon = \pi/4$, $\Psi = \pi/4$, and $r = 150$ Mpc. with the same noise spectral densities for all detectors.

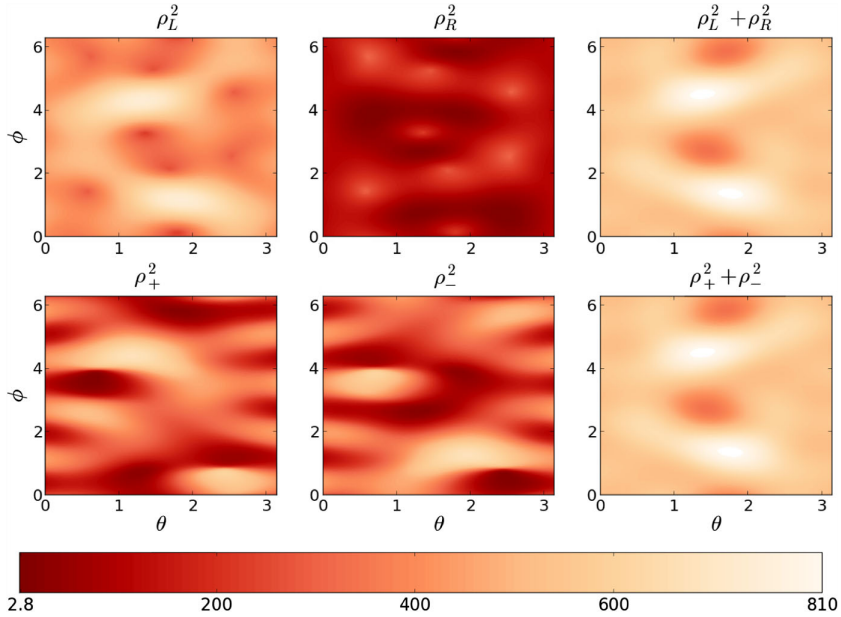

FIG. 3 (color online). Directional SNR squares $\boldsymbol{\rho}_L^2, \boldsymbol{\rho}_R^2, \boldsymbol{\rho}_+^2, \boldsymbol{\rho}_-^2$, and $\boldsymbol{\rho}^2{}_{\rm net}$ for network LHVKI with $m_1, m_2 = 1.4$, $\epsilon = \pi/4$, $\Psi = \pi/4$, and $r = 150$ Mpc, with the same noise spectral densities for all detectors.

distinct pairs of synthetic streams, Eqs. (34) and (54). This can be understood as follows.

We recall that the network SNR vector $\boldsymbol{\varrho}$ is located in the complex 2-plane formed by the vectors $\mathbf{d}$ and $\mathbf{d}^*$ as in Eq. (8). In general any orthogonal complex vector pair which spans this 2-plane would capture the norm of $\boldsymbol{\varrho}$. The above-mentioned synthetic stream pairs $\mathbf{z}_{L,R}$ as defined in Eq. (34) and $\mathbf{z}_\pm$ as defined in Eq. (54) are constructed using two different pairs of real orthogonal vectors, namely;,$\{\mathbf{F}'^{DP}_{+,\times}\}$ and $\{\mathsf{v}_\pm\}$, respectively. Below, we give the expressions for these real vectors as the linear combinations of $\mathbf{d}$ and $\mathbf{d}^*$,

$$\mathbf{F}'^{DP}_{+} = \Re[\mathbf{d}e^{-i\frac{\delta}{2}}], \qquad \mathbf{F}'^{DP}_{\times} = \Im[\mathbf{d}e^{-i\frac{\delta}{2}}], \tag{56}$$

$$\mathsf{v}_+ = \Re[\mathbf{d}e^{-i\alpha}], \qquad \mathsf{v}_- = \Re[\mathbf{d}e^{i\alpha}], \tag{57}$$

with $\alpha = \frac{1}{2}\cos^{-1}[-\frac{|\mathbf{d}^{\rm T}\mathbf{d}|\cos\delta}{\mathbf{d}^{\rm H}\mathbf{d}}]$ and $\delta = \arg(\mathbf{d}^T\mathbf{d})$ as defined earlier.

In the following figures, we pictorially compare the SNRs of the two synthesis stream pairs, $\boldsymbol{\rho}_{L,R}$ and $\boldsymbol{\rho}_\pm$, as well as the network SNR $\boldsymbol{\rho}$ for different multidetector networks. We consider the binary system with component masses $(1.4, 1.4)M_\odot$, polarization $\psi = \pi/4$ and inclination $\epsilon = \pi/4$ located at the distance of 150 Mpc. For this exercise we consider various networks with constituent detectors LIGO-Livingston (L), LIGO-Hanford (H), Virgo (V), KAGRA (K), and the detector in India denoted by (I).[12] We assume all the detectors with a "zero-detuning, high-power" Advanced LIGO noise curve given by Eq. (4.7) of Ref. [29]. Figure 1 gives the SNRs corresponding to three representative 3-detector networks, namely, LVH, LVI, and LHI. Similarly Fig. 2 is for three 4-detector networks LHVK, LHVI, and LVKI, and Fig. 3 is for a 5-detector network LHVKI.

Several distinct features are noted in the SNR figures of the two synthetic stream pairs. As expected the total network SNR square for both the pairs is the same, namely, $\boldsymbol{\rho}_L^2 + \boldsymbol{\rho}_R^2 = \boldsymbol{\rho}_+^2 + \boldsymbol{\rho}_-^2 = \boldsymbol{\rho}^2$. Please see the corresponding pannels in Figs. 1, 2, and 3. In most of the cases, $\boldsymbol{\rho}_L$ is higher than $\boldsymbol{\rho}_R$, and it carries the features of the network SNR, $\boldsymbol{\rho}$. In the case of $\boldsymbol{\rho}_\pm$ pairs, on average the network SNR seemed to have distributed between the ρ_+ and ρ_-more or less equally. These features can be used to construct a consistency test for the targeted directional search, which we are currently investigating.

VII. CONCLUSION

The interferometric multidetector GW network can be described as a pair *effective* multidetector antennas which captures most of the features of multidetector coherent analysis. The number 2 pertains to the two polarizations of Einstein's gravity.

In past, the multidetector coherent compact binary coalescence inspiral MLR analysis was formulated by various groups, in particular Ref. [11] using Gel–Fand functions and Ref. [13] using the $\mathcal{F}$ statistic. In both these works, the network LLR was maximized over four extrinsic parameters $(\mathrm{A}_0, \phi_a, \epsilon, \Psi)$ and the network maximum LLR statistic was obtained. It was noted that maximum LLR statistic can be interpreted in terms of two synthetic

[12]Hypothetically we take Pune, India, as the location for the detector in India.

streams, which are linear combinations of the overwhitened data from individual detectors with directional network dependent coefficients pertaining to the two polarizations. Thus, the synthetic streams emerge in the MLR statistic only after the maximization. However, since in Einstein's gravity a GW carries two polarizations, it is more natural to expect two effective data streams (independent of the detection statistic) to capture the polarizations when we have more than one detector.

In this work, we have derived the network synthetic data streams much before the construction of LLR statistic using the matching filtering idea applied to the network data and the singular-value-decomposition technique applied to the network SNR vector. These streams individually capture the two circular polarizations. Then, the network LLR naturally emerges as the sum of the LLRs of the synthetic streams. The four physical parameters, namely, $(\mathrm{A}_0, \phi_a, \epsilon, \Psi)$ get mapped to two amplitude and two phase parameters pertaining to the circular polarizations in the signal. The MLR analysis over these new parameters $(\boldsymbol{\rho}_L, \boldsymbol{\rho}_R, \Phi_L, \Phi_R)$ is a straightforward task.

The DP frame is a specific choice of wave frame in which the the real and imaginary parts of noise weighted complex network antenna pattern vector becomes orthogonal to each other. We have demonstrated that the dominant polarization frame naturally emerges out of the SVD of the SNR vector.

Connecting this work to the existing literature, namely, Refs. [11] and [13], we explicitly show that the two synthetic streams discussed in the earlier works are distinct, and they can be related through the network constructs. In both the works, the authors use a pair of orthonormal complex vectors which span the $\mathbf{d}$-$\mathbf{d}^*$ complex plane to construct two synthetic data streams. Though the choice of the basis vector pairs, which span the two-dimensional complex plane, are different, the total network SNR is the same. This work aims to combine all the existing formalisms of the multidetector pertaining to the compact binary coalescence and show that the two synthetic streams can be obtained using the network SNR vector.

The above formalism allows us to study the properties of the network synthetic streams more effectively. The multidetector SNR can be decomposed into two pieces pertaining to two synthetic stream SNRs, which individually carry the multidetector features. We are currently investigating the properties of these streams and their individual contribution in the angular resolution improvement in the multidetector context. Another direction we are investigating is to use their properties in the inspiraling binary search, namely, to develop the consistency tests as well as to carry out an efficient all-sky search with a global detector network.

ACKNOWLEDGMENTS

This work is supported by AP's SERC Fast Track Scheme For Young Scientists. H. K. thanks Albert Einstein Institute, Hannover, for hospitality for a stay during which part of the manuscript writing was carried out. The authors would like to thank S. Fairhurst, B. S. Santhyaprakash, Gianluca Guidi, I. Harry, and Shubhanshu Tiwari for useful discussion and helpful comments on this work. The authors would also like to thank the anonymous reviewer for the thorough review and very helpful feedback. The main result of this work is presented in the LIGO-Virgo Scientific Meeting at Hannover, 2013 (LIGO laboratory Document No. LIGO-G1301109). This document has been assigned LIGO laboratory Document No. LIGO-P1300229.

APPENDIX A: LIKELIHOOD RATIO

The network log likelihood ratio is

$$\Lambda = \sum_{m=1}^{I} \langle \mathbf{x}_m | \mathbf{s}_m \rangle - \frac{1}{2} \langle \mathbf{s}_m | \mathbf{s}_m \rangle = \sum_{m=1}^{I} 4\Re \left[\sum_{j=1}^{N} \tilde{\tilde{\mathcal{X}}}_{jm} \tilde{\mathcal{S}}^*_{jm} \right] - 2 \left[\sum_{j=1}^{N} \frac{|\tilde{\mathcal{S}}_{jm}|^2}{\mathcal{N}_{jm}} \right]. \quad \text{(A1)}$$

We use Eq. (34) to express the network LLR in terms of $(P_L, P_R, \Phi_L, \Phi_R)$, and we get

$$\sum_{m=1}^{I} 4\Re \left[\sum_{j=1}^{N} \tilde{\tilde{\mathcal{X}}}_{jm} \tilde{S}^*_{jm} \right] = 4\mathrm{A}_0 \mathrm{P}_L \Re \left[\sum_{j=1}^{N} \sum_{m=1}^{I} \tilde{\tilde{\mathcal{X}}}_{jm} \mathrm{F}^{DP}_{+m} \tilde{h}^*_{0j} e^{-i\Phi_L} \right] + 4\mathrm{A}_0 \mathrm{P}_R \Re \left[\sum_{j=1}^{N} \sum_{m=1}^{I} \tilde{\tilde{\mathcal{X}}}_{jm} \mathrm{F}^{DP}_{\times m} \tilde{h}^*_{0j} e^{-i\Phi_R} \right] = \mathrm{A}_0 [\mathrm{P}_L \| \mathbf{F}'^{DP}_{+} \| \langle \mathbf{z}_L | \mathbf{h}_0 e^{i\Phi_L} \rangle + \mathrm{P}_R \| \mathbf{F}'^{DP}_{\times} \| \langle \mathbf{z}_R | \mathbf{h}_0 e^{i\Phi_R} \rangle]. \quad \text{(A2)}$$

Equations (13) and (16) give

$$\mathrm{A}_0 \mathrm{P}_L \| \mathbf{F}'^{DP}_{+} \| = \boldsymbol{\rho}_L, \qquad \mathrm{A}_0 \mathrm{P}_R \| \mathbf{F}'^{DP}_{\times} \| = \boldsymbol{\rho}_R. \quad \text{(A3)}$$

Also, from Eq. (7) one can easily show that the second terms in Eq. (A1) are half of network SNR square, $\boldsymbol{\rho}_L^2 + \boldsymbol{\rho}_R^2$.

Substituting back in Eq. (A1),

$$2\Lambda = [2\boldsymbol{\rho}_L \langle \mathbf{z}_L | \mathbf{h}_0 e^{i\Phi_L} \rangle - \boldsymbol{\rho}_L^2] + [2\boldsymbol{\rho}_R \langle \mathbf{z}_R | \mathbf{h}_0 e^{i\Phi_R} \rangle - \boldsymbol{\rho}_R^2]. \quad \text{(A4)}$$

APPENDIX B: RELATION BETWEEN OLD AND NEW EXTRINSIC PARAMETERS

The maximum log likelihood ratio is obtained by maximizing the network LLR over the four extrinsic parameters, which are the functions of physical parameters $(\mathrm{A}_0, \phi_a, \epsilon, \Psi)$. As we discussed earlier, the choice of these functions depends on the formalism. In this appendix,

we relate the extrinsic parameter set $(\mathrm{A}_0, \phi_a, \epsilon, \Psi)$ with $(\mathcal{A}_1, \mathcal{A}_2, \mathcal{A}_3, \mathcal{A}_4)$.

The extrinsic parameters used in this paper are

$$\begin{aligned}
\boldsymbol{\rho}_L &= \mathrm{A}_0 \|\mathbf{F}_+^{DP}\| \sqrt{\left(\frac{1+\cos^2\epsilon}{2}\right)^2 \cos^2 2\chi + \cos^2\epsilon \, \sin^2 2\chi}, \\
\boldsymbol{\rho}_R &= \mathrm{A}_0 \|\mathbf{F}_2^{DP}\| \sqrt{\left(\frac{1+\cos^2\epsilon}{2}\right)^2 \sin^2 2\chi + \cos^2\epsilon \, \cos^2 2\chi}, \\
\Phi_L &= \tan^{-1}\left[\tan(2\chi)\frac{2\cos\epsilon}{1+\cos^2\epsilon}\right] + \phi_a, \\
\Phi_R &= \tan^{-1}\left[-\cot(2\chi)\frac{2\cos\epsilon}{1+\cos^2\epsilon}\right] + \phi_a.
\end{aligned} \tag{B1}$$

In Ref. [13], the maximization of LLR is done over a set of derived amplitude parameters,

$$\begin{aligned}
\mathcal{A}_1 &= \mathrm{A}_0\left[\frac{1+\cos^2\epsilon}{2}\cos\phi_a \cos 2\Psi - \cos\epsilon \, \sin\phi_a \sin 2\Psi\right], \\
\mathcal{A}_2 &= \mathrm{A}_0\left[\frac{1+\cos^2\epsilon}{2}\cos\phi_a \sin 2\Psi + \cos\epsilon \, \sin\phi_a \cos 2\Psi\right], \\
\mathcal{A}_3 &= \mathrm{A}_0\left[-\frac{1+\cos^2\epsilon}{2}\sin\phi_a \cos 2\Psi - \cos\epsilon \, \cos\phi_a \sin 2\Psi\right], \\
\mathcal{A}_4 &= \mathrm{A}_0\left[-\frac{1+\cos^2\epsilon}{2}\sin\phi_a \sin 2\Psi + \cos\epsilon \, \cos\phi_a \cos 2\Psi\right].
\end{aligned} \tag{B2}$$

These are related to $(\boldsymbol{\rho}_L, \boldsymbol{\rho}_R, \Phi_L, \Phi_R)$ as follows:

$$\begin{aligned}
(\mathcal{A}_1 - i\mathcal{A}_3)\cos\frac{\delta}{2} + (\mathcal{A}_2 - i\mathcal{A}_4)\sin\frac{\delta}{2} &= \frac{\boldsymbol{\rho}_L}{\|\mathbf{F}'^{DP}_+\|} e^{i\Phi_L}, \\
(\mathcal{A}_2 - i\mathcal{A}_4)\cos\frac{\delta}{2} - (\mathcal{A}_1 - i\mathcal{A}_3)\sin\frac{\delta}{2} &= \frac{\boldsymbol{\rho}_R}{\|\mathbf{F}'^{DP}_\times\|} e^{i\Phi_R}.
\end{aligned} \tag{B3}$$

This implies

$$\begin{aligned}
\mathcal{A}_1 &= \frac{\boldsymbol{\rho}_L}{\|\mathbf{F}'^{DP}_+\|}\cos\frac{\delta}{2}\cos\Phi_L - \frac{\boldsymbol{\rho}_R}{\|\mathbf{F}'^{DP}_\times\|}\sin\frac{\delta}{2}\cos\Phi_R, \\
\mathcal{A}_2 &= \frac{\boldsymbol{\rho}_L}{\|\mathbf{F}'^{DP}_+\|}\sin\frac{\delta}{2}\cos\Phi_L + \frac{\boldsymbol{\rho}_R}{\|\mathbf{F}'^{DP}_\times\|}\cos\frac{\delta}{2}\sin\Phi_R, \\
\mathcal{A}_3 &= -\frac{\boldsymbol{\rho}_L}{\|\mathbf{F}'^{DP}_+\|}\cos\frac{\delta}{2}\sin\Phi_L + \frac{\boldsymbol{\rho}_R}{\|\mathbf{F}'^{DP}_\times\|}\sin\frac{\delta}{2}\sin\Phi_R, \\
\mathcal{A}_4 &= -\frac{\boldsymbol{\rho}_L}{\|\mathbf{F}'^{DP}_+\|}\sin\frac{\delta}{2}\sin\Phi_L - \frac{\boldsymbol{\rho}_R}{\|\mathbf{F}'^{DP}_\times\|}\cos\frac{\delta}{2}\sin\Phi_R.
\end{aligned} \tag{B4}$$

For Eq. (B4), the map between $(\mathrm{A}_0, \phi_a, \epsilon, \Psi)$ and $(\mathcal{A}_1, \mathcal{A}_2, \mathcal{A}_3, \mathcal{A}_4)$ is one to one.

APPENDIX C: LIKELIHOOD ESTIMATES OF POLARIZATION ANGLES

As we discussed earlier, a network of detectors can recover the polarization information of GW. Since $\mathbf{z}_L$ and $\mathbf{z}_R$ are the equivalent detectors of the network, we can obtain the estimates of polarization angles $\hat{\epsilon}$ and $\hat{\Psi}$ in terms of their SNRs. By using Eqs. (13) and (16) and the definition of $\Phi_{L,R}$, we define

$$\begin{aligned}
Y \equiv \frac{\boldsymbol{\rho}_L \|\mathbf{F}_\times^{DP}\| \mathbf{e}^{i\Phi_L}}{\boldsymbol{\rho}_R \|\mathbf{F}_+^{DP}\| \mathbf{e}^{i\Phi_R}} &= \frac{\cos 2\chi \frac{1+\cos^2\epsilon}{2} + i \sin 2\chi \cos\epsilon}{\sin 2\chi \frac{1+\cos^2\epsilon}{2} - i \cos 2\chi \cos\epsilon} \\
&= i\frac{T^*_{2+2}(\chi,\epsilon,0) + T^*_{2-2}(\chi,\epsilon,0)}{T^*_{2+2}(\chi,\epsilon,0) - T^*_{2-2}(\chi,\epsilon,0)}.
\end{aligned} \tag{C1}$$

This implies

$$\frac{T_{2-2}(\chi,\epsilon,0)}{T_{2+2}(\chi,\epsilon,0)} = \frac{iY^* - 1}{iY^* + 1}. \tag{C2}$$

Then polarization angles can be expressed in terms of Y as follows:

$$\begin{aligned}
\cos 4\Psi &= \cos\left[\arg\left(\frac{T_{2-2}}{T_{2+2}}\right) + \delta\right] \\
&= \cos\left[\arg\left(\frac{iY^* - 1}{iY^* + 1}\right) + \delta\right],
\end{aligned} \tag{C3}$$

and

$$\cos\epsilon = \frac{1 - \sqrt{\left|\frac{T_{2-2}}{T_{2+2}}\right|}}{1 + \sqrt{\left|\frac{T_{2-2}}{T_{2+2}}\right|}} = \frac{1 - \sqrt{\left|\frac{iY^*-1}{iY^*+1}\right|}}{1 + \sqrt{\left|\frac{iY^*-1}{iY^*+1}\right|}}. \tag{C4}$$

However, when the noise is present, $\boldsymbol{\rho}_L, \boldsymbol{\rho}_R, \Phi_L, \Phi_R$ are estimated using the MLR approach. Then using Eq. (C1), Y is constructed out of $\hat{\boldsymbol{\rho}}_L, \hat{\boldsymbol{\rho}}_R, \hat{\Phi}_L, \hat{\Phi}_R$ estimates. Thus, $(\hat{\epsilon}, \hat{\Psi})$ is obtained by Eqs. (C3) and (C4), with newly constructed Y.

[1] G. M. Harry (LIGO Scientific Collaboration), Classical Quantum Gravity **27**, 084006 (2010).
[2] The Virgo Collaboration, Tech. Rep. VIR-0027A-09, https://tds.ego-gw.it/ql/?c=6589.
[3] K. Somiya (KAGRA Collaboration), Classical Quantum Gravity **29**, 124007 (2012).
[4] J. Abadie *et al.* (LIGO Scientific Collaboration, Virgo Collaboration), Classical Quantum Gravity **27**, 173001 (2010).
[5] S. Kay, *Fundamentals of Statistical Signal Processing, Vol II-Detection Theory* (Prentice Hall, New Jersey, 1998).
[6] B. J. Owen and B. S. Sathyaprakash, Phys. Rev. D **60**, 022002 (1999).
[7] B. S. Sathyaprakash and S. V. Dhurandhar, Phys. Rev. D **44**, 3819 (1991).
[8] S. Babak *et al.*, Phys. Rev. D **87**, 024033 (2013).
[9] H. Mukhopadhyay, N. Sago, H. Tagoshi, S. Dhurandhar, H. Takahashi, and N. Kanda, Phys. Rev. D **74**, 083005 (2006).
[10] S. Fairhurst, New J. Phys. **11**, 123006 (2009).
[11] A. Pai, S. Dhurandhar, and S. Bose, Phys. Rev. D **64**, 042004 (2001).
[12] L. S. Finn, Phys. Rev. D **63**, 102001 (2001).
[13] I. W. Harry and S. Fairhurst, Phys. Rev. D **83**, 084002 (2011).
[14] P. Jaranowski, A. Królak, and B. F. Schutz, Phys. Rev. D **58**, 063001 (1998).
[15] C. Cutler and B. F. Schutz, Phys. Rev. D **72**, 063006 (2005).
[16] S. Klimenko, S. Mohanty, M. Rakhmanov, and G. Mitselmakher, Phys. Rev. D **72**, 122002 (2005).
[17] J. Sylvestre, Phys. Rev. D **68**, 102005 (2003).
[18] A. Pai, E. Chassande-Mottin, and O. Rabaste, Phys. Rev. D **77**, 062005 (2008).
[19] S. K. Saha, *Aperture Synthesis: Methods and Applications to Optical Astronomy* (Springer, New York, 2010).
[20] J. D. Monnier, Rep. Prog. Phys. **66**, 789 (2003).
[21] D. Keppel, arXiv:1307.4158.
[22] K. G. Arun, B. R. Iyer, B. S. Sathyaprakash, and P. A. Sundararajan, Phys. Rev. D **71**, 084008 (2005).
[23] B. F. Schutz, arXiv:gr-qc/9710080.
[24] Y. Gürsel and M. Tinto, Phys. Rev. D **40**, 3884 (1989).
[25] The very large telescope interferometer, http://www.eso.org/paranal/telescopes/vlti/.
[26] Very-long-baseline interferometry, http://en.wikipedia.org/wiki/Very-long-baseline_interferometry.
[27] S. Dhurandhar and M. Tinto, Mon. Not. R. Astron. Soc. **234**, 663 (1988).
[28] M. Maggiore, *Gravitational Waves: Volume 1: Theory and Experiments* (Oxford University, New York, 2008).
[29] P. Ajith, Phys. Rev. D **84**, 084037 (2011).